

SELF-ALIGNED PROTON IMPLANTATION GaAs MESFET DEVICES

C.Lanzieri, P.D'Eustacchio, M.Peroni, A.Cetronio
ALENIA S.p.A., Direzione Ricerche, Via Tiburtina, Roma, Italy
G.Ghione and M.Pirola

Politecnico di Torino, Dipartimento di Elettronica, Corso Duca degli Abruzzi, Torino, Italy
A.Carnera and A.Gasparotto
Università di Padova, Dipartimento di Fisica, Padova, Italy

ABSTRACT

In this work we will demonstrate that Self Aligned Proton Implantation (SAPI) devices give excellent transconductance linearity (i.e. virtually constant at approximately 150 mS/mm for drain current in the range I_{dss} to 15% I_{dss}) and increased output resistance. Said devices, with a $0.5 \times 300 \mu\text{m}$ gate geometry, typically yield 1.6 dB noise figure and 9.0 dB associated gain at 12 GHz.

INTRODUCTION

Even though the importance of an abrupt active-channel/semi-insulating substrate interface for improved GaAs MESFET output resistance and transconductance linearity is well known, because of technological limitations, investigations to date (both theoretical and experimental) have been limited to p/n or GaAlAs/GaAs total channel interface structures fabricated by ion-implantation and/or epitaxial growth techniques. Nevertheless as indicated by theoretical simulation of ion-implanted MESFET devices with different interface structures, notable improvement in device performance can be achieved when a localised abrupt interface structure is positioned under the gate metalisation.

By utilising the well known property of hydrogenation [1] already used in MESFET fabrication [2], to selectively neutralise the shallow donors under the gate metalisation to form an abrupt interface, appreciable improvement in MESFET devices can be achieved.

In this article we will present theoretical and experimental results of ion-implanted MESFET devices with and without a localised n/n⁻ abrupt interface under the gate metalisation. The latter structure, self-aligned to the gate, is obtained by compensating the $^{29}\text{Si}^+$ donor profile tail with an appropriate proton implantation prior to gate recessing and metalisation, and a post-proton implant stabilisation phase to ensure complete and irreversible compensation of the donor profile tail.

EXPERIMENTAL

Semi-insulating (S.I.) GaAs wafers were selectively ion implanted with $^{29}\text{Si}^+$ to a dose of $1.4 \times 10^{13} \text{ cm}^{-2}$ at 100 keV and thereafter annealed in a conventional furnace at 820°C for 20 minutes in the presence of reactively sputter deposited Si_3N_4 encapsulating film. As shown in fig.1 after ohmic contact and gate lithography realisation the substrates are subjected to selective proton (H^+) implantation under the gate with a dose and energy (i.e. $1.5 \times 10^{12} \text{ cm}^{-2}$ at 50 keV) sufficient to neutralise the donor implant tail at the active layer/semi-insulating substrate interface.

After proton implantation and channel recessing the devices are completed by means of a conventional MESFET processing technology comprising: Al gate metalisation and lift-off, Si_3N_4 passivation and Ti/Pt/Au overlayer metalisation. In order to stabilise the devices and eventually reduce any mis-orientation effects in the doped GaAs layer a low temperature anneal at 350°C for one hour is carried out.

In addition to the MESFET devices appropriate test structures for Hall resistivity measurements are also fabricated to enable characterisation of the selectively proton implanted $^{29}\text{Si}^+$ tails.

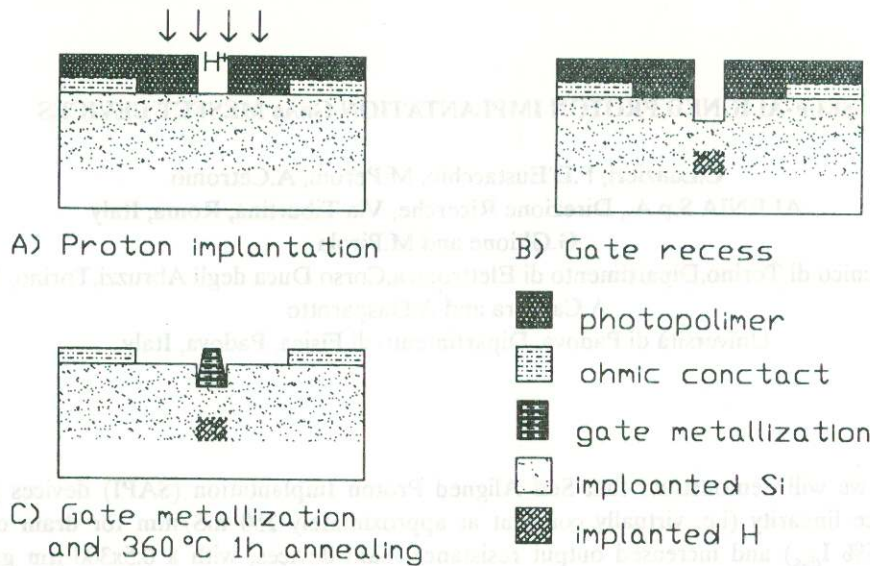


Fig. 1 Schematic representation of SAPI-MESFET fabrication steps prior to passivation and overlayer deposition.

Characterisation of the implanted layer.

In order to estimate the implanted H^+ distribution in the $^{29}Si^+$ implanted GaAs substrate before and after the stabilising anneal, appropriate samples implanted as above, have been submitted for SIMS analysis. In order to reduce the background noise during the these measurements deuterium ($^2H^+$) has been used. Because the chemical and implantation properties of $^2H^+$ are known to be similar to H^+ [3] a study of the former isotope should give a good indication of the proton distribution.

As revealed by SIMS analysis the as implanted $^2H^+$ distribution is in good agreement with TRIM [4] simulations whereas after thermal annealing the $^2H^+$ is redistributed towards the peak and tail of the Si distribution is good agreement with other reported results which indicate hydrogen accumulation in regions with high defect and impurity concentration [5].

In order to evaluate the effect of proton implantation on the free carrier concentration and mobility profile, Differential Hall measurements [6] on Van der Pauw samples before and after proton implantation and stabilisation anneal have been carried out.

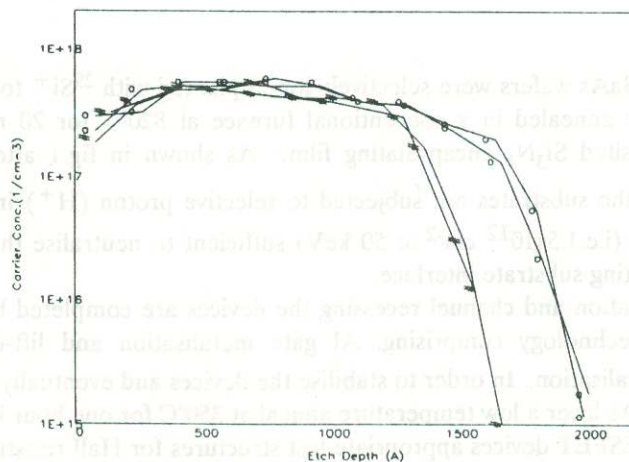


Fig. 2 Hall free carrier concentration profiles for proton implanted and conventional Silicon donor profiles.

As shown in fig.2 the electron concentration profile in the hydrogenated sample is appreciably shorter and steeper, indicating that donor compensation is very effective at the active layer/semi-insulating substrate interface. The electron saturation drift velocity deduced from drain saturation current versus recess depth measurements, in conjunction with the concentration profiles in fig.2, indicated that hydrogenated and non hydrogenated samples have the same drift velocity, which in the plateau region of the concentration profile is approximately 1×10^7 cm/s.

Device Simulation

Numerical simulations have been used for the evaluation not only of the realised devices, but also for an estimation of the performances of a totally proton implanted channel device. The same channel and buffer mobility has been supposed for all the simulated devices. The estimation of the activated dopant profiles for the simulation of the conventional and proton-implanted FETS have been deduced from the differential Hall measurements results presented in fig.2. For all the devices simulated, I_{dss} was assumed to be 200 mA/mm in agreement with the fabrication (trimming) procedure: Said approach results in slightly different recess depths for the three devices i.e. 815 Å for the conventional MESFET, 720 Å for the total channel H^+ implant and 730 Å for the SAPI device.

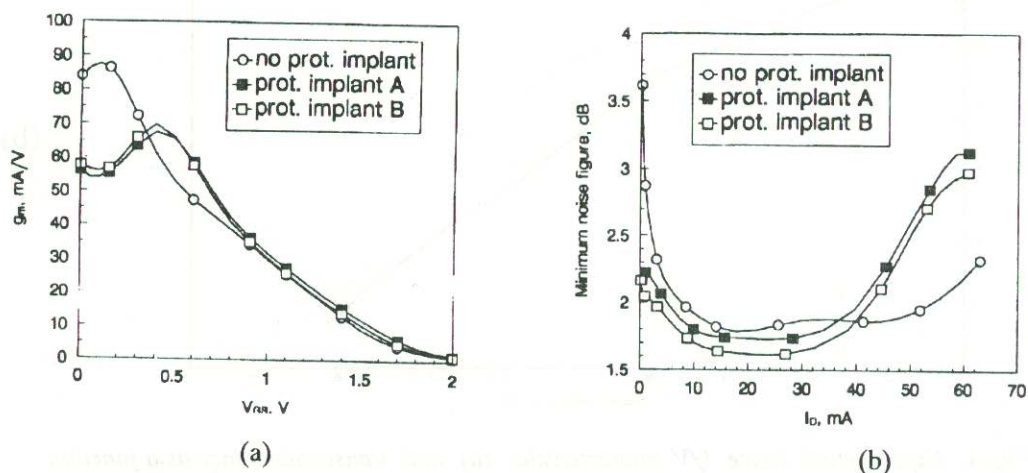


Fig. 3 Simulated device transconductance (a) and low noise performance (b) as a function of drain current (A) total H^+ implant and (B) SAPI.

As shown in fig.3a, the transconductance (g_m) behaviour of the simulated devices produces an increased g_m linearity both for the SAPI-MESFET and the total proton implanted channel device. Nevertheless even though not shown in fig.3 the source and drain resistances for the latter device also increase (i.e. $R_s = 1.6 \Omega$ and $R_d = 2.6 \Omega$ for SAPI and $R_s = 2.0 \Omega$ and $R_d = 3.2 \Omega$ for total channel H^+ implant), and this slightly degrades the overall device performance, as shown by the noise figure simulation is fig. 3b. In terms of output resistance, all three devices are fairly similar with $R_{ds} = 350 \Omega$.

Device characteristics

In fig.4a are presented typical I/V characteristic for the SAPI and conventional MESFET devices, which clearly indicate the basic differences between the two devices. In particular we observe that:

- in the SAPI device looping of the I/V characteristics is appreciably reduced, indicating a reduction of defect states at the doped channel /semi-insulating substrate interface [7];

- ii) an increase in drain conductance of the SAPI device; simulated results gave a similar output resistance for both devices; said discrepancy with experimental results can be attributed to deep trap effects not included in the simulation;
- iii) improved transconductance linearity for the SAPI device as a result of the compensated donor tail. As shown by a more detailed representation in fig. 4b, for the latter device the transconductance remains constant at approximately 150 mS/mm from I_{dss} to approx. 15% I_{dss} .

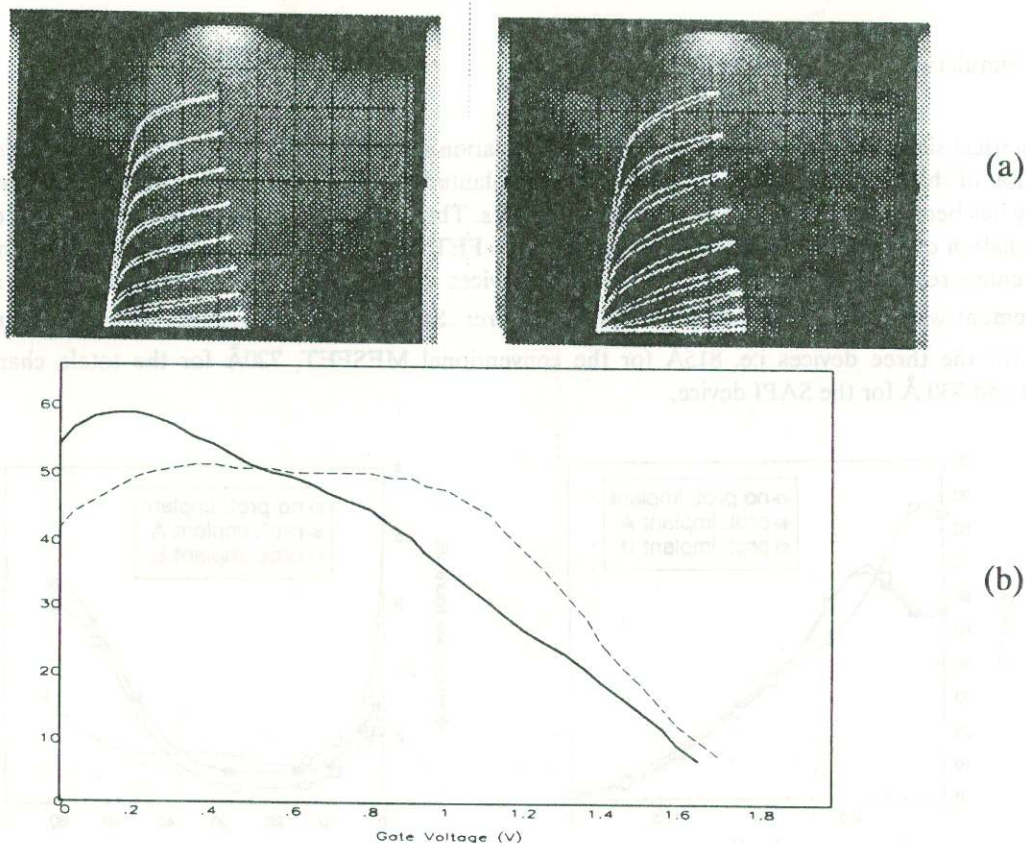


Fig. 4 Experimental device I/V characteristics (a) and transconductance as a function of gate voltage (b) for conventional (—) and SAPI (---) MESFETS.

As shown in table 1, the above observations are confirmed by the device intrinsic equivalent circuit parameters obtained from S-parameters measurements. In fact the major differences between the two devices are, a higher transconductance (g_m), output resistance (R_{ds}) and input capacitance (C_{gs}) of the SAPI device in low-noise bias conditions (i.e. 15% I_{ds}). The performance benefits of higher g_m and R_{ds} are in device maximum available gain (MAG) and low-noise associated gain (G_{ass}). In particular for the SAPI device the $MAG \approx 11$ dB and $G_{ass} \approx 9$ dB at 12 GHz whereas for the corresponding conventional MESFET the $MAG \approx 9$ dB and $G_{ass} \approx 7$ dB. The higher SAPI transconductance at low-noise bias does not improve its noise behaviour as a result of the corresponding increase in device input capacitance. In fact both devices yield a noise figure of approximately 1.6 dB at 12 GHz.

Because the stability of proton implanted devices can be of some concern we have carried out preliminary high temperature storage tests to evidentiate this point. In particular we have controlled the saturation current, pinch-off voltage and input capacitance of a batch of 20 devices during high temperature storage at 200°C. To date, after approximately 1500 hrs of storage there appears to be no stability differences between the SAPI and conventional MESFET devices, with parameters variations better than $\pm 2\%$.

| SAPI (conventional) | DEVICE BIAS CONDITIONS | | |
|----------------------------------|------------------------|----------------|---------------|
| | I_{dss} | 50% I_{dss} | 15% I_{dss} |
| g_m (mS) | 57 (79) | 55 (56) | 40 (32) |
| C_{gs} (pF) | .46 (.47) | .44 (.35) | .36 (.26) |
| C_{gd} (pF) | .038 (.039) | .039 (.041) | .04 (.045) |
| R_{ds} (Ohm) | 270 (153) | 271 (180) | 278 (209) |
| Noise Figure at 12GHz (dB) | | | 1.6 (1.6) |
| Associated Gain at 12GHz (dB) | | | 8.5 (7.5) |

Table 1 Equivalent circuit parameters for SAPI and conventional MESFET devices.

CONCLUSIONS

A technologically simple approach based on a self aligned proton implantation under the gate region has been presented. The MESFET devices fabricated with this technique have shown excellent transconductance linearity and increased output resistance. Preliminary storage tests at 200°C indicate device stability comparable with conventional MESFET devices.

REFERENCES

- 1) J. Chevallier, W.C Dautermon-Smith, C.W. Tu and S.J. Pearton, *Appl. Phys. Lett.* vol.47, p.108, 1985.
- 2) E. Constant, N. Caglio, J. Chevallier and J. C. Pesant, *Electron. Lett.* Vol.23, p.841, 1987.
- 3) R.G.Wilson, D.A.Betts, D.K.Sadana, J.M.Zavada, R.G.Hunsperger, *J.Appl. Phys.* Vol 57, p.5006, 1985.
- 4) J.F.Ziegler, J.P.Biersack and U.Littmark, "The Stopping and Range of Ions in Solids", Pergamon Press (N.Y), 1985.
- 5) J. M. Zavada, R. G. Wilson and J. Comas, *J. Appl. Phys.* Vol 65, p.1968, 1989.
- 6) T. Ambridge and C. J. Allen, *Electron. Lett.* Vol.15, p.648, 1979.
- 7) Ladbrooke and Blight, *IEEE Trans. El. Dev.* Vol.35, p.257, 1985.
- 8) M.S. Shur, *IEEE Trans. El. Dev.* Vol.32, p.18, 1988.